*Journal of Organometallic Chemistry*, 438 (1992) 159–165
Elsevier Sequoia S.A., Lausanne
JOM 22821

# Electrochemical behaviour of *trans*-[FeH(CNR)(dppe)$_2$]$^+$. Kinetic parameters determined by digital simulation of cyclic voltammetry

M. Amélia N.D.A. Lemos and Armando J.L. Pombeiro
*Centro de Química Estrutural, Complexo I, Instituto Superior Técnico, 1096 Lisboa Codex (Portugal)*

(Received February 27, 1992)

**Abstract**

A new digital simulation program, based on the box method, has been developed and applied to the cyclic voltammetric ECECE anodic behaviour of *trans*-[FeH(CNR)(dppe)$_2$]$^+$ (R = Me, Et, $^t$Bu, $C_6H_4$Me-4, $C_6H_4NO_2$-4, or $C_6H_4$OMe-4; dppe = $Ph_2PCH_2CH_2PPh_2$), allowing us to estimate relevant kinetic parameters, in particular the homogeneous rate constant for electroinduced proton loss upon metal–hydride bond cleavage. This is shown to correlate with the electron donor/acceptor properties of the *trans* isocyanide ligand, as expressed by the electrochemical $P_L$ ligand parameter, and the Taft $\sigma^*$ polar constant (for the alkyl isocyanides) or the Hammett $\sigma_p^+$ constant (for the aromatic isocyanides).

## Introduction

Cyclic voltammetry is a very useful technique for examining the mechanisms involved in redox reactions and the properties and behaviour of the intervening species [1,2]. However, due to the dynamic character of the experiment, it is rather difficult to obtain an accurate estimate of the kinetic parameters for these reactions.

The current availability of computational techniques and the rapid development of microcomputer technology has provided useful tools to analyse cyclic voltammetric data. In particular, digital simulation, which requires the simultaneous solution of the diffusion equations for all the species involved, has evolved rapidly in recent years and a variety of methods has been proposed to integrate the corresponding differential equations [3–6].

In the present study we have applied such techniques to the {FeH(dppe)$_2$}$^+$ centre (dppe = $Ph_2PCH_2CH_2PPh_2$), which is able to bind dinitrogen and a variety of other related ligands, such as isocyanides [7].

Correspondence to: Professor A.J.L. Pombeiro.

We have shown earlier that $[FeH(CNMe)(dppe)_2]^+$ undergoes a complex oxidation process, exhibiting, by cyclic voltammetry at sufficiently low scan rates, two anodic waves separated by about 200 mV. The first wave involves the transfer of two electrons and, in the presence of $BF_4^-$, leads to the new fluoro-complex $[FeF(CNMe)(dppe)_2]^+$ [8]. The second wave corresponds to the oxidation of this fluoro-complex, which has been isolated and characterized. The use of published simulation data (from ref. 9) and of digital simulation, has enabled us to propose the following ECECE-type reaction mechanism, which involves the oxidation of the original complex and the subsequent loss of a proton from the oxidized species, forming an unstable iron(I) complex that is rapidly oxidized and attacked by the tetrafluoroborate ion to yield the final complex (see Scheme 1).

$$[FeH(CNR)(dppe)_2]^+ \overset{-e^-}{\rightleftharpoons} [FeH(CNR)(dppe)_2]^{2+} \xrightarrow{-H^+}$$

$$[Fe(CNR)(dppe)_2]^+ \overset{-e^-}{\rightleftharpoons} [Fe(CNR)(dppe)_2]^{2+} \xrightarrow{+F^-}$$

$$[FeF(CNR)(dppe)_2]^+ \overset{-e^-}{\rightleftharpoons} [FeF(CNR)(dppe)_2]^{2+}$$

Scheme 1. Reaction scheme for the oxidation of the complexes $[FeH(CNR)(dppe)_2]^+$.

The extension of this study to a range of CNR ligands (R = Me, Et, $^t$Bu, $C_6H_4$Me-4, $C_6H_4NO_2$-4 or $C_6H_4$OMe-4), which we also report here, allows us further to investigate the electron-acceptor/donor characteristics of the iron centre, relating electrochemical data to the properties of the ligands.

## Experimental procedures and digital simulation

All the compounds were prepared from $[FeHCl(dppe)_2]$ by addition of a chloride abstractor ($TlBF_4$ or $TlPF_6$) and the required isocyanide. A series of complexes with the general formula $[FeH(CNR)(dppe)_2]A$ (R = Me, Et, $^t$Bu, $C_6H_4$Me-4, $C_6H_4NO_2$-4, or $C_6H_4$OMe-4; A = $BF_4$ or $PF_6$) was prepared. Experimental details are described elsewhere [7].

Cyclic voltammograms were obtained at room temperature, in a 0.2 M solution of $[Bu_4N][BF_4]$ in tetrahydrofuran (THF), at a platinum wire working-electrode, with a silver wire pseudo-reference electrode connected by a Luggin capillary to the cell. A platinum auxiliary electrode was employed. An EG&G PARC model 175 programmer and model 173 potentiostat were used, and the voltammograms were recorded in a Houston 2000 XY recorder. Controlled potential electrolysis was carried out in an H-type cell, with two compartments separated by a glass frit, and with platinum gauze working- and counter-electrodes in the same electrolyte solution and using an EG&G PARC model 179 coulometer. A Luggin capillary probing the working-electrode was connected to a silver wire pseudo-reference-electrode.

The peak potentials of the complexes are quoted relative to SCE by using as internal reference the $[Fe(\eta^5\text{-}C_5H_5)_2]^{0/+}$ couple ($E^{ox}_{1/2}$ = 0.545 V *vs.* SCE). All the experiments were performed under dinitrogen or argon.

Digital simulation was carried out by the box method and the use of an appropriate numerical technique to integrate the equations. Two integration methods were tried, the classical Runge–Kutta 4th method and a multi-step predictor-corrector one [10,11]. Since the latter proved to be much more accurate

and fast, this was used for the final results. The equations were solved using the Adams–Bashforth predictor formula coupled to the Adams–Moulton corrector. With a well chosen step the corrector formula was only used once and provided a reliable estimate of the error in each step. Since multi-step methods are not self-starting, 4th order Runge–Kutta was used as a starter.

To obtain digitally simulated voltammograms a program was written in Turbo Pascal®, Version 6.0 (Borland International). The program is highly structured and the mechanism-dependent code is self-contained to permit simple changes to the simulated mechanism.

The program was run on an IBM-compatible personal computer equipped with a 80386SX/25 MHz processor and a FasMath Cyrix mathematics coprocessor.

Experimental voltammograms were digitized with a Graphtec KD 3300 digitizer tablet.

In order to fit the simulated voltammograms to the experimental results, the values of the heterogeneous rate constants ($k^0$) and the standard potentials ($E^0$) for the first and third redox couples as well as the homogeneous rate constant for the rate-limiting chemical reaction ($k_{hom}$) were varied to give a general best fit. The homogeneous rate constant for the fluorination reaction is higher than maximum attainable rate range, and was taken as infinite. The heterogeneous rate constant ($k^0$(II)) and potential ($E^0$(II)) for the second redox couple, corresponding to the iron(I) species, were kept at 0.01 cm/s and 0 V respectively. This potential is sufficiently less than the first couple that no influence on the simulated voltammogram should be detected, regardless of its actual value [9,12]. The values for $\alpha$ were kept constant at 0.5. When necessary, the experimental voltammograms were baseline-corrected for the background oxidation of the electrolyte solution. This correction was particularly important for the complexes with the highest oxidation potentials.

## Results and discussion

All the alkylisocyanide complexes of this series show a common cyclic voltammetric pattern: a first anodic wave (wave I), reversible only at scan rates higher than 500 mV/s (Table 1), followed by a second reversible wave (wave II), at a higher potential, well defined only at slow scan rates (below 200 mV/s) (Fig. 1). The arylisocyanide complexes also show two anodic waves but at higher potentials, with no observable cathodic counterpart for the first wave regardless of the scan rate (Fig. 2).

Table 1

Peak potentials for the first and the second anodic waves of *trans*-[FeH(CNR)(dppe)$_2$]$^+$ observed at 100 mV/s

| R | $E_p$(I) [a] (V) | $E_p$(II) [a] (V) | R | $E_p$(I) [a] (V) | $E_p$(II) [a] (V) |
|---|---|---|---|---|---|
| Me | 0.93 | 1.05 | $C_6H_4$Me-4 | 1.00 | 1.14 |
| Et | 0.93 | 1.05 | $C_6H_4NO_2$-4 | 1.08 | 1.32 |
| $^t$Bu | 0.92 | 1.07 | $C_6H_4$OMe-4 | 0.97 | 1.09 |

[a] Values (±20 mV) relative to SCE.

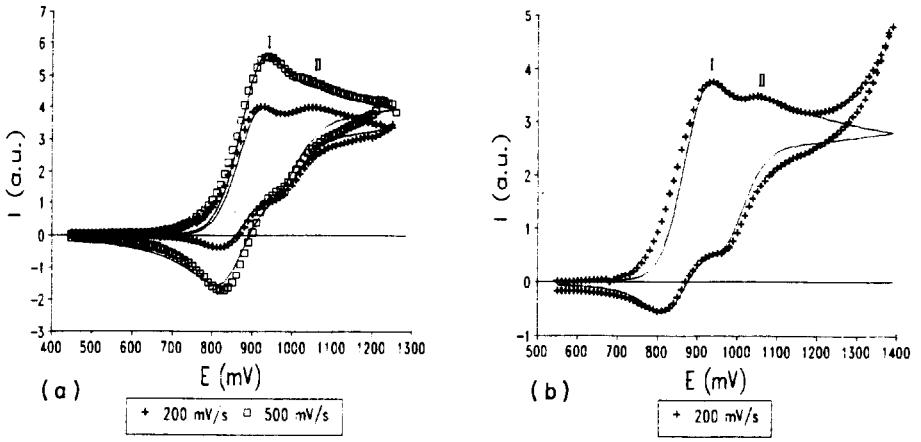


Fig. 1. Cyclic voltammograms for the alkyl isocyanide complexes *trans*-$[FeH(CNR)(dppe)_2]^+$ [R = Me (a) and Et (b)]. Symbols are experimental points and lines are the simulated voltammograms. Current (I) is in arbitrary units.

The current-function for the first wave corresponds to two electrons at slower scan rates (controlled potential electrolyses confirmed this and to a single electron at higher scan rates). The electrosynthesized product at the first anodic wave of the methylisocyanide complex was isolated and characterized as the fluoro-isocyanide complex. It has a one-electron reversible oxidation (confirmed by controlled potential electrolysis) at the potential corresponding to the second cyclic voltammetry wave of a solution of the parent complex.

The observations are consistent with the ECECE mechanism proposed in Scheme 1.

Figures 1 and 2 also show the best-fit simulated curves corresponding to typical voltammograms and Table 2 summarizes the parameters obtained for these systems.

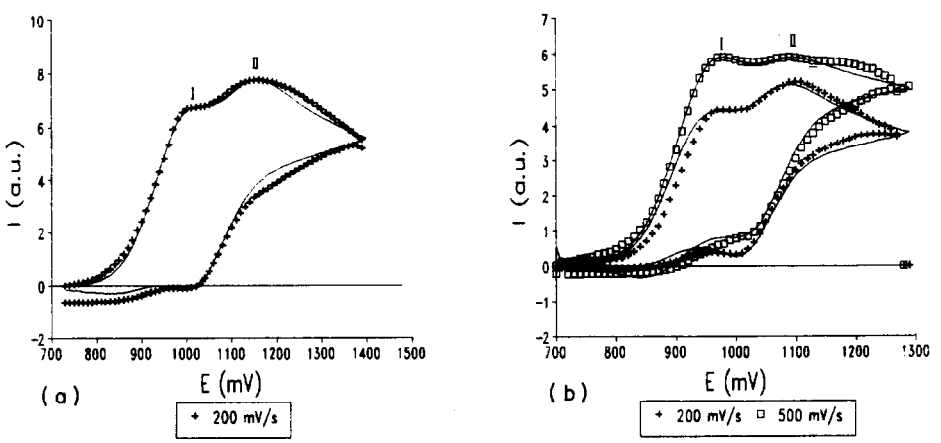


Fig. 2. Cyclic voltammograms for the aryl isocyanide complexes *trans*-$[FeH(CNR)(dppe)_2]^+$ [R = $C_6H_4Me$-4 (a) or $C_6H_4OMe$-4 (b)]. Symbols are experimental points and lines are the simulated voltammograms.

Table 2

Estimated standard redox potentials ($E^0$) and homogeneous rate constants ($k_{hom}$) for the electrode processes occurring in cyclic voltammetry of the *trans*-[FeH(CNR)(dppe)$_2$]$^+$ complexes

| R | $E^0$(I) [a] (mV) | $k^0$(I)$\times 10^2$ (cm/s) | $E^0$(III) [a] (mV) | $k^0$(III)$\times 10^2$ (cm/s) | $k_{hom}$ (s) |
|---|---|---|---|---|---|
| Me | 870 | 0.9 | 1005 | 1 | 0.9 |
| Et | 868 | 0.6 | 1005 | 1 | 0.6 |
| $^t$Bu | 780 | 0.1 | 1010 | 0.5 | 0.25 |
| $C_6H_4$Me-4 | 910 | 0.45 | 1080 | 0.7 | 5 |
| $C_6H_4NO_2$-4 | 1030 | 1 | 1215 | 2 | 9 |
| $C_6H_4$OMe-4 | 890 | 0.6 | 1045 | 2 | 1.9 |

[a] Values (±20 mV) relative to SCE.

There is a significant difference between the behaviour of the complexes of aliphatic and aromatic isocyanides. This difference is due mainly to the higher rate for the homogeneous reaction that occurs when the isocyanide ligand possesses an aromatic ring, and is associated with the better electron-acceptor capacity of such a ligand.

With aliphatic isocyanides the homogeneous rate constant appears to increase in the order $^t$Bu < Et < Me, thus following the decrease of the electron-donor capacity of R.

For ligands having an aromatic ring, the homogeneous rate constant depends on the *para* substituent (see below).

These observations can be explained by the fact that the reaction involves loss of a proton, which is enhanced by increase of electron-accepting ability of the isocyanide ligand.

*Correlations*

The results obtained can be correlated with semi-empirical parameters that are used to measure the net electron acceptor/donor character of the ligands, such as $P_L$ [1], Hammett $\sigma_p$ (for ligands containing a *para*-substituted aromatic ring) or Taft $\sigma^*$ (for isocyanides with an aliphatic R group).

Figure 3 shows that the standard redox potentials for the first and the third redox couples, as well as the natural logarithm of the homogeneous rate constant, correlate roughly with $P_L$, which increases with the net difference of $\pi$-electron acceptor and $\sigma$-donor abilities.

The best fitting straight lines are indicated by eqs. 1–3 (R = 0.94, 0.99, 0.91, respectively) (for potentials in V and $k_{hom}$ in $s^{-1}$).

$$E^0(\mathrm{I}) = 1.59 + 1.73\ P_L \quad (1)$$

$$E^0(\mathrm{III}) = 1.79 + 1.81\ P_L \quad (2)$$

$$\ln(k_{hom}) = 11 + 27\ P_L \quad (3)$$

A comparison of these equations can be made with the original approach [1] where $P_L$ is correlated with the half-wave potential $E_{1/2}$ (eq. 4) where $E_s$ is the electron-richness and $\beta$ the polarisability of the metal site.

$$E_{1/2} = E_s + \beta P_L \quad (4)$$

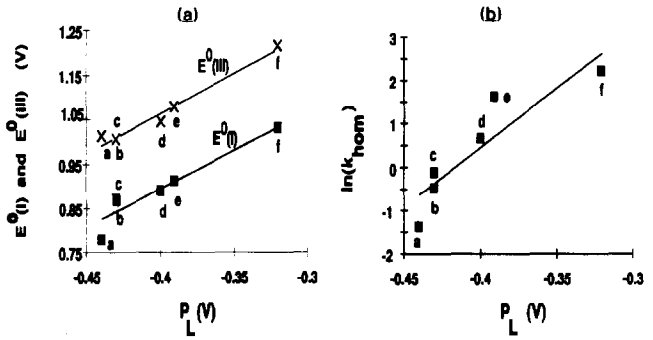


Fig. 3. Plot of $E^0$ for the first (squares) and the third (crosses) redox couples (a) and of the natural logarithm of the homogeneous rate constant (b) *versus* $P_L$. [R = $^t$Bu (a), Et (b), Me (c), $C_6H_4OMe$-4 (d), $C_6H_4Me$-4 (e), $C_6H_4NO_2$-4 (f).]

The litercept in the above equations represents the electron-richness ($E_s$) of the binding metal site, and therefore the fluoride site $\{FeF(dppe)_2\}^+$ is electron-poorer than $\{FeH(dppe)_2\}^+$. The slope should be the polarisability ($\beta$) of the metal site and the two metal centres have similar values of this parameter.

The literature parameters for the hydride metal site [1] ($E_s = 1.04$ V; $\beta = 1.0$ V) differ from those reported here. Although this can be related to the fact that we are using $E^0$ while the original correlation used $E_{1/2}$ (the corresponding values show only a constant deviation for reversible systems), it also suggests that the $P_L$ values of the isocyanides at the iron centre are different from those defined [1] (and used in this study) for the standard $\{Cr(CO)_5\}$ site; this is in agreement with the previously observed [14] dependence of $P_L$ (for isocyanides) on the binding metal centre.

The redox potentials and the homogeneous rate constant (natural logarithm) increase with the Taft polar $\sigma^*$ constant or the Hammett's $\sigma_P^+$ constant [13] (Fig. 4), suggesting direct conjugation between the aryl substituents and the redox centre, and its determining role in the proton loss step. Moreover, a related correlation was observed [14] in the case of the redox potential for the series

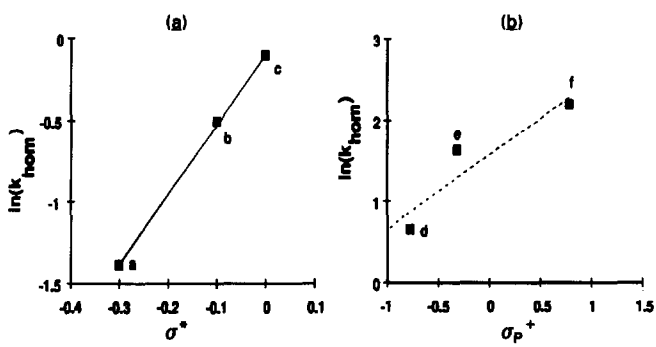


Fig. 4. Plot of the natural logarithm of the homogeneous rate constant *versus* $\sigma^*$ (for ligands with an aliphatic R group) (a), and *versus* $\sigma_P^+$ (for ligands with a *para* substituted aromatic ring) (b). [R = $^t$Bu (a), Et (b), Me (c), $C_6H_4OMe$-4 (d), $C_6H_4Me$-4 (e), $C_6H_4NO_2$-4 (f)].

*trans*-[ReCl(CNR)(dppe)$_2$]. The best least-square fits are given by eqs. 5 and 6 (R = 1 and 0.93, respectively).

$$\ln(k_{hom}) = 1.6 + 0.9\sigma_P^+ \quad (5)$$

$$\ln(k_{hom}) = -0.1 + 4.3\sigma^* \quad (6)$$

## Conclusions

The cyclic voltammetric behaviour of the hydride-isocyanide can be explained in terms of the anodic ECECE mechanism proposed [8] for the methylisocyanide species [FeH(CNMe)(dppe)$_2$]$^+$. It was possible to estimate the kinetic parameters for this process, which has previously been achieved in only a rather limited number of cases [15].

The standard redox potential for their oxidation ($E^0$(I)), as well as for the fluoride complexes ($E^0$(III)), and the homogeneous rate constant for proton loss reaction correlate with parameters that indicate a considerable interaction between the hydride and the *trans* isocyanide ligand. This is mainly determined by polar effects, within the alkylisocyanide series, or by direct conjugation between the ring substituent and the redox metal centre for the aromatic isocyanide complexes.

## Acknowledgements

This work has been partially supported by JNICT and INIC. We also thank Dr. C. Amatore for valuable and stimulating discussions.

## References

1 J. Chatt, C.T. Kan, G.J. Leigh, C.J. Pickett and D.R. Stanley, J. Chem. Soc., Dalton Trans., (1980) 2032.
2 C.P. Andrieux, P. Hapiot and J.-M. Saveant, Chem. Rev., 90 (1990) 723.
3 D. Britz, Digital Simulation in Electrochemistry, Springer-Verlag, Berlin, 1988.
4 D.K. Gosser and F. Zhang, Talanta, 38(7) (1991) 715.
5 S.W. Feldberg, J. Electroanal. Chem., 290 (1990) 49.
6 M. Rudolph, J. Electroanal. Chem., 292 (1990) 1.
7 M.B. Baptista, M.A.N.D.A. Lemos, J.J.R. Fraústo da Silva and A.J.L. Pombeiro, J. Organomet. Chem., in press.
8 M.A.N.D.A. Lemos and A.J.L. Pombeiro, J. Organomet. Chem., 332 (1987) C17, M.A.N.D.A. Lemos and A.J.L. Pombeiro, Portugaliae Electrochim. Acta, 9 (1991) 171.
9 R.S. Nicholson and I. Shain, Anal. Chem., 37(2) (1965) 178.
10 A. Constantinides, Applied Numerical Methods with Personal Computers, McGraw-Hill, New York, 1987.
11 S.D. Conte and C. de Boor, Elementary Numerical Analysis, 2nd ed., McGraw Hill, New York, 1972.
12 D.S. Polcyn and I. Shain, Anal. Chem., 38(3) (1966) 370.
13 C. Laurence and B. Wojtkowiak, Ann. Chim., 5 (1970) 163.
14 A.J.L. Pombeiro, C.J. Pickett and R.L. Richards, J. Organomet. Chem., 224 (1982) 285.
15 G. Kokkinidis, G. Papanastasiou, C. Hasiotis and N. Papadopoulos, J. Electroanal. Chem., 309 (1991) 263.